View Online / Journal Homepage / Table of Contents for this issue

Organic & Biomolecular Chemistry

Dynamic Article Links

Cite this: *Org. Biomol. Chem.*, 2012, **10**, 640

www.rsc.org/obc

PAPER

β-Phenylproline: the high β-turn forming propensity of proline combined with an aromatic side chain†‡

Paola Fatás, Ana I. Jiménez,* M. Isabel Calaza and Carlos Cativiela*

Received 12th September 2011, Accepted 5th October 2011
DOI: 10.1039/c1ob06561k

Published on 05 October 2011 on http://pubs.rsc.org | doi:10.1039/C1OB06561K
Downloaded by Universitaire d'Angers on 08 February 2012

The conformational propensities of the proline analogue bearing a phenyl substituent attached to the β carbon, in either a *cis* or a *trans* configuration relative to the carbonyl group, have been investigated. The behaviour of *cis*- and *trans*(βPh)Pro has been compared with that of proline in homochiral and heterochiral dipeptide sequences. NMR and IR studies as well as X-ray diffraction analysis provide evidence that the β-phenyl substituent does not disrupt the tendency of proline to occupy the *i*+1 position of a β-turn. The puckering of the pyrrolidine ring is significantly affected by the presence of the aromatic substituent, which tends to occupy positions that minimize steric repulsions. As a consequence, this substituent adopts specific well-defined orientations, which are more restricted for the *cis* derivative. Interactions between this aromatic group and that in the adjacent phenylalanine residue may be responsible for some of the conformational differences observed among the different peptides studied.

Introduction

The applications of peptides in medicine and other fields rely on the three-dimensional arrangement of their main-chain and side-chain functionalities. Great efforts have been devoted in the last decades to developing methods to efficiently control the folding mode of the peptide backbone.[1] Among them is the incorporation of non-proteinogenic residues whose structure has been designed to stabilize certain conformations among those energetically accessible to the coded amino acids.[1,2]

Proline is the only proteinogenic amino acid that exhibits limited conformational flexibility and a marked propensity to explore only a few regions of the Ramachandran map.[3,4] Due to its cyclic structure, rotation around the C^{α}–N bond is forbidden and, as a consequence, proline can only adopt a narrow range of ϕ values ($\approx -60°$). This is at the basis of the well-known tendency of proline to act as a turn inductor and, in particular, to occupy the *i*+1 position of β-turns.[4,5] The unique structure of proline may serve as inspiration for the construction of novel amino acids with well-defined conformational propensities. Such proline-based residues may incorporate modifications aimed at fine-tuning the conformational properties of the parent amino acid or at the addition of new side-chain functionalities. Among the latter is the attachment of a substituent to the pyrrolidine β carbon to generate an analogue bearing the side chain of another proteinogenic amino acid. This is the case with β-phenylproline, (βPh)Pro (Fig. 1), which can be regarded as a proline–phenylalanine hybrid in which the orientation of the aromatic substituent is dictated by the conformation of the five-membered ring and the *cis* or *trans* configuration of the phenyl group relative to the carbonyl moiety. Accordingly, *cis*(βPh)Pro and *trans*(βPh)Pro combine the conformational properties of proline with an aromatic side-chain functionality that is rigidly oriented with respect to the peptide backbone, and this may be useful in the design of biologically active peptides and other applications relying on specifically-oriented side-chain moieties.

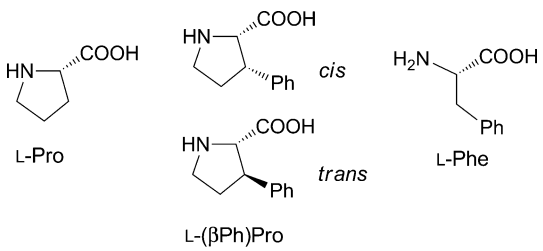

Fig. 1 Comparison of the structures of proline and phenylalanine with those of the hybrid amino acid β-phenylproline, (βPh)Pro. The aromatic side chain in the latter may exhibit a *cis* or a *trans* configuration relative to the carboxylic acid group.

(βPh)Pro has been inserted into a number of bioactive peptides[6] as a replacement for either proline or phenylalanine and has led to

Departamento de Química Orgánica, ISQCH, Universidad de Zaragoza–CSIC, 50009 Zaragoza, Spain. E-mail: anisjim@unizar.es, cativiela@unizar.es

† This article is part of an Organic & Biomolecular Chemistry web theme issue on Foldamer Chemistry.

‡ Electronic supplementary information (ESI) available: Complete list of geometrical parameters for the X-ray structures, copies of ^{1}H-NMR, ^{13}C-NMR and NOESY spectra of **1–4**, and characterization data for the precursors **1a–4a**. CCDC reference numbers 842881–842885. For ESI and crystallographic data in CIF or other electronic format see DOI: 10.1039/c1ob06561k

This journal is © The Royal Society of Chemistry 2012

Published on 05 October 2011 on http://pubs.rsc.org | doi:10.1039/C1OB06561K
Downloaded by Universitaire d'Angers on 08 February 2012

enhanced peptide-receptor affinity and improved stability in some cases. Although some of these studies have used computational methods to try to rationalise the biological activity observed as a function of the structural modification performed,[6a,d] the conformational propensities of (βPh)Pro have not been established to date. This can be best achieved through the in-depth analysis of small model peptides that incorporate this amino acid. In the present work, the ability of *cis*(βPh)Pro and *trans*(βPh)Pro to induce a β-turn when occupying the *i*+1 position of a dipeptide sequence has been evaluated and compared to that of the natural amino acid. Although several β-substituted proline analogues other than (βPh)Pro have been the subject of structural studies (mainly, as diamide derivatives),[7] the formation of β-turns has been addressed only in a few cases,[8] in which other amino acids with restricted conformational properties either coded (proline)[8c,d] or not (*N*-methyl or cyclopropaneamino acids)[8a,b] were present. In this work, (βPh)Pro is combined with phenylalanine, a residue with no specific conformational bias. This allows the evaluation of very subtle structural aspects and a precise comparison of the behaviour of (βPh)Pro and proline as β-turn inductors. The conformation adopted by the (βPh)Pro-containing model peptides has been established in solution and in the solid state using different spectroscopic techniques and X-ray diffraction studies.

Results and discussion

To explore the ability of (βPh)Pro to induce a β-turn conformation, both the *cis* and *trans* stereoisomers of this amino acid were inserted in the *i*+1 position of two peptide sequences differing in the chirality of the *i*+2 residue, namely RCO-L-Pro*-L-Phe-NHR′ and RCO-L-Pro*-D-Phe-NHR′, where Pro* stands for *cis* and *trans* (βPh)Pro as well as for the natural amino acid, L-Pro. In all cases, the (βPh)Pro residues exhibiting an *S* stereochemistry at the α carbon (equivalent to an L configuration) were considered, that is, (2*S*,3*S*)(βPh)Pro for the *cis* derivative and (2*S*,3*R*)(βPh)Pro for the *trans* isomer (note that the α and β carbons correspond to positions 2 and 3 of the pyrrolidine ring, respectively). To help comparison with the natural amino acid, these residues will be termed L-*cis*(βPh)Pro and L-*trans*(βPh)Pro, respectively, all through the text.

The terminally blocked dipeptides RCO-L-Pro*-L-Phe-NHR′ and RCO-L-Pro*-D-Phe-NHR′ are adequate models to study the formation of β-turns of types I and II. As stated in the *Introduction* section, the ϕ dihedral of proline (defining rotation about the N–C^{α} bond) is confined to around –60°. The ψ torsion angle (C^{α}–C′ torsion) has been shown to prefer values around –30° or 140°.[3,4] Accordingly, proline is overwhelmingly found in the (–60,–30) and (–60,140) regions of the Ramachandran map.[3,4] These (ϕ,ψ) angles are very close to the ideal values corresponding to the *i*+1 position of a β-turn of type I or II,[5,9] respectively, which explains the high propensity of proline to induce these folding modes. The presence of an L or D residue in the *i*+2 position (as L-Phe or D-Phe in the sequences selected for study) entails a preference for the type I or II β-turn in the absence of intermolecular interactions,[5,10] as seen below. The two β-turn types differ mainly in the orientation of the central peptide bond (that formed by the Pro-C′O and Phe-NH moieties), which is rotated by nearly 180°.[5,9]

Enantiomerically pure L-*cis*(βPh)Pro bearing the amino function protected with a *tert*-butoxycarbonyl (Boc) group was coupled with L- or D-phenylalanine-*N*′-methylamide (H-L-Phe-NHMe or H-D-Phe-NHMe) through activation with BOP[11] [(benzotriazol-1-yloxy)tris(dimethylamino)phosphonium hexafluorophosphate]. The resulting dipeptides **1a** and **2a** were treated with a solution of hydrogen chloride in ethyl acetate to remove the Boc group and subsequently acylated with pivaloyl chloride to afford, respectively, Piv-L-*cis*(βPh)Pro-L-Phe-NHMe (**1**) and Piv-L-*cis*(βPh)Pro-D-Phe-NHMe (**2**) (Piv = pivaloyl, *t*BuCO) (Fig. 2). Following an identical procedure, enantiomerically pure L-*trans*(βPh)Pro was transformed into Piv-L-*trans*(βPh)Pro-L-Phe-NHMe (**3**) and Piv-L-*trans*(βPh)Pro-D-Phe-NHMe (**4**) (Fig. 2) through the *N*-Boc-protected intermediates **3a** and **4a**.

Compounds **1** and **3** are characterized by a homochiral sequence (L-L) and their behaviour is to be compared with that of the analogous dipeptide containing the natural amino acid, Piv-L-Pro-L-Phe-NHMe (**5**). In a similar way, Piv-L-Pro-D-Phe-NHMe (**6**) serves as model for the heterochiral (L-D) dipeptides **2** and **4**. The conformational propensities of the two L-Pro-containing peptides have previously been established in detail, both in the solid state[10,12] and in solution.[10,13]

The four dipeptides **1**–**4** and the *N*-Boc precursor **4a** provided single crystals suitable for X-ray diffraction analysis.‡ Their molecular structures are shown in Fig. 3–7. Two independent molecules (A, B) were found in the asymmetric unit of **3**, **4** and **4a**. All the compounds crystallised adopt a β-turn stabilised by an intramolecular hydrogen bond that links the terminal methylamide NH and pivaloyl or Boc C′O group and closes a ten-membered cycle. The distances and angles for this intramolecular hydrogen-bond interaction are within the range 2.86–2.95 Å (N···O) and 151–161° (N–H···O).[14] Table 1 lists the main backbone torsion angles. Those corresponding to the pyrrolidine ring and the phenyl substituent in (βPh)Pro as well as to the benzyl side chain of L/D-Phe are given in Table 2. A complete list of geometrical parameters is provided as ESI.‡ The data in Tables 1 and 2 show that the

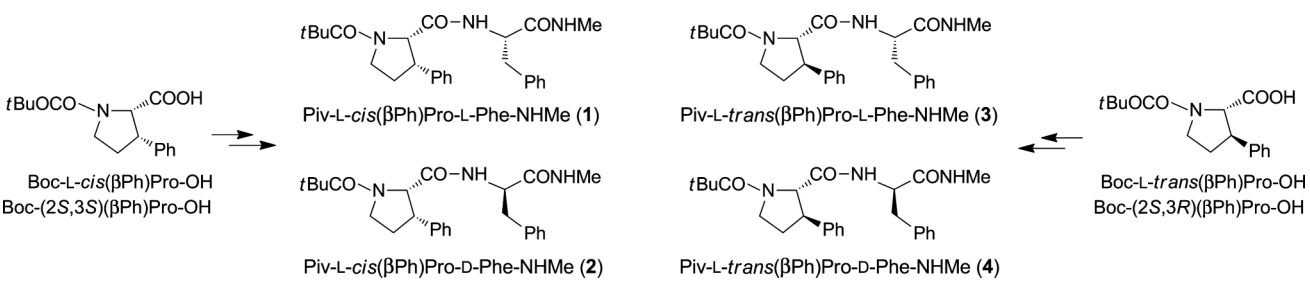

Fig. 2 Structure of dipeptides **1**–**4** that incorporate the *cis* or *trans* stereoisomer of L-(βPh)Pro in position *i*+1. Abbreviations: Boc = *tert*-butoxycarbonyl; Piv = pivaloyl (*tert*-butylcarbonyl).

Published on 05 October 2011 on http://pubs.rsc.org | doi:10.1039/C1OB06561K
Downloaded by Universitaire d'Angers on 08 February 2012

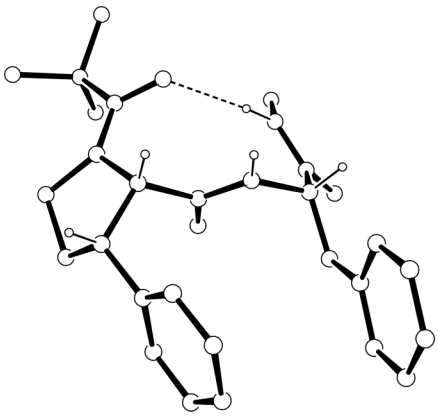

Fig. 3 Crystal molecular structure of Piv-L-*cis*(βPh)Pro-L-Phe-NHMe (**1**). Only the hydrogens linked to nitrogen or chiral carbon atoms are shown. The intramolecular hydrogen bond is indicated by a dashed line.

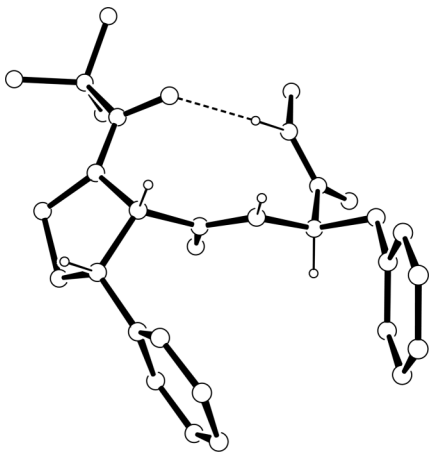

Fig. 4 Crystal molecular structure of Piv-L-*cis*(βPh)Pro-D-Phe-NHMe (**2**). Only the hydrogens linked to nitrogen or chiral carbon atoms are shown. The intramolecular hydrogen bond is indicated by a dashed line.

two independent molecules in **3**, **4** and **4a** exhibit quite similar backbone conformations while differing in the arrangement of the side chain moieties.

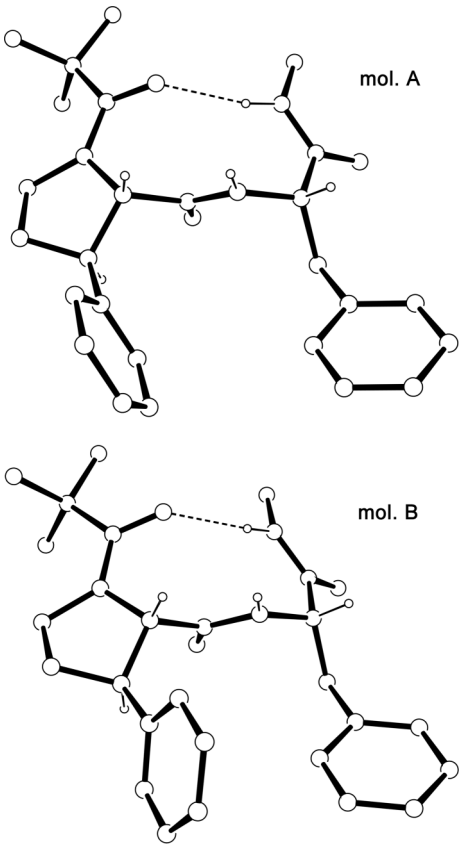

Fig. 5 Crystal molecular structure of Piv-L-*trans*(βPh)Pro-L-Phe-NHMe (**3**) (two independent molecules: A, B). Only the hydrogens linked to nitrogen or chiral carbon atoms are shown. The intramolecular hydrogen bond is indicated by a dashed line.

All the amide bonds are found[14] in the usual *trans* conformation ($\omega \approx 180°$), including the urethane in **4a**, with only slight deviations from planarity except for that involving the pivaloyl group in **2** ($\omega = 171°$). Not surprisingly, the torsion angles in Table 1 correspond in all cases to a β-turn of type II, as previously observed in the solid state for the reference compounds **5** and **6**.[10,12] In this disposition, the (βPh)Pro C^{α}–H and Phe N–H bonds are parallel and point in the same direction (Fig. 3–7). All the (βPh)Pro

Table 1 Main backbone torsion angles[a] (deg) in the X-ray diffraction structures of dipeptides **1–4** and **4a**.[b] Those reported for the analogous compounds containing L-Pro (**5**, **6**) are included for comparison

			Pro*[c]		Phe	
Peptide			ϕ	ψ	ϕ	ψ
Piv-L-*cis*(βPh)Pro-L-Phe-NHMe	**1**		−60	130	52	35
Piv-L-*cis*(βPh)Pro-D-Phe-NHMe	**2**		−62	134	62	26
Piv-L-*trans*(βPh)Pro-L-Phe-NHMe	**3**	mol. A	−53	132	64	19
		mol. B	−56	135	60	25
Piv-L-*trans*(βPh)Pro-D-Phe-NHMe	**4**	mol. A	−58	128	72	5
		mol. B	−60	128	91	−11
Boc-L-*trans*(βPh)Pro-D-Phe-NHMe	**4a**	mol. A	−56	127	86	4
		mol. B	−55	131	81	0
Piv-L-Pro-L-Phe-NHMe[d]	**5**		−64	139	62	23
Piv-L-Pro-D-Phe-NHMe[e]	**6**		−57	138	72	12

[a] For standard deviations, see the ESI.‡ [b] The asymmetric unit of **3**, **4** and **4a** contains two independent molecules (A, B). [c] Pro* refers to Pro or the corresponding (βPh)Pro stereoisomer. [d] From ref. 10. [e] From ref. 12.

 This journal is © The Royal Society of Chemistry 2012

Published on 05 October 2011 on http://pubs.rsc.org | doi:10.1039/C1OB06561K
Downloaded by Universitaire d'Angers on 08 February 2012

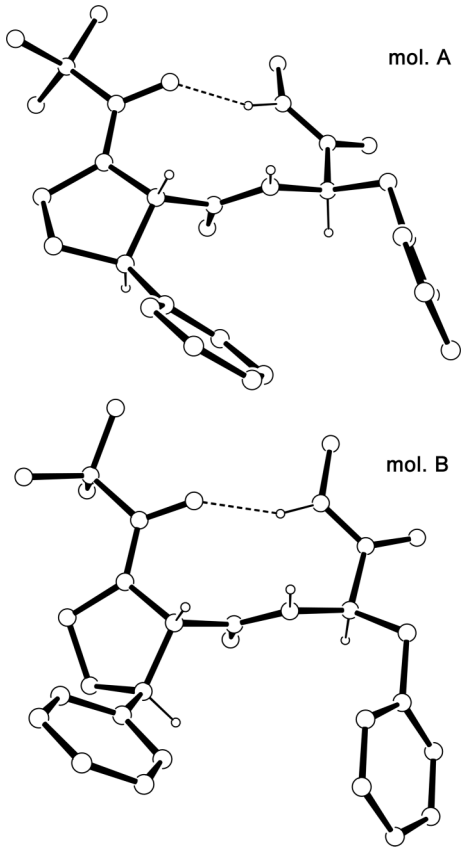

Fig. 6 Crystal molecular structure of Piv-L-*trans*(βPh)Pro-D-Phe-NHMe (**4**) (two independent molecules: A, B). Only the hydrogens linked to nitrogen or chiral carbon atoms are shown. The intramolecular hydrogen bond is indicated by a dashed line.

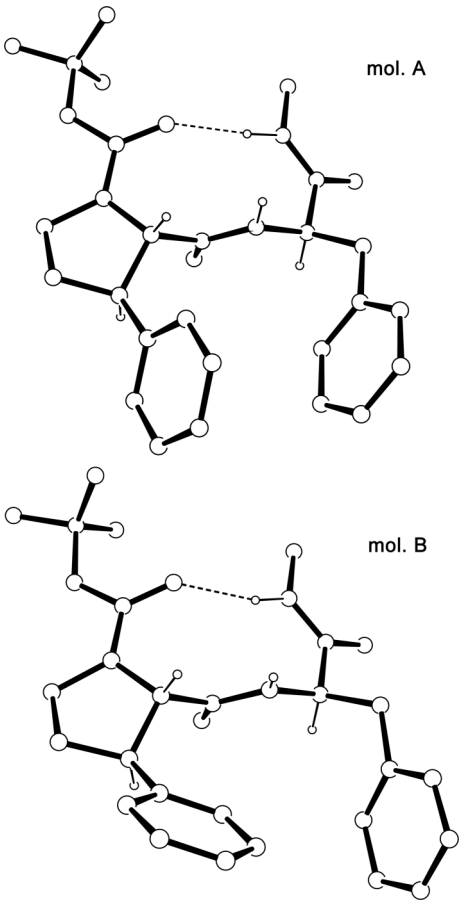

Fig. 7 Crystal molecular structure of Boc-L-*trans*(βPh)Pro-D-Phe-NHMe (**4a**) (two independent molecules: A, B). Only the hydrogens linked to nitrogen or chiral carbon atoms are shown. The intramolecular hydrogen bond is indicated by a dashed line.

residues in the crystallised molecules, whatever the *cis* or *trans* stereochemistry, display (ϕ,ψ) values near (–60,130) (Table 1), that is, very close to those considered ideal for the *i*+1 position of a βII-turn,[5,9] (–60,120). This suggests that the additional β-phenyl substituent in the pyrrolidine ring does not hamper the orientation of the adjacent carbonyl moiety leading to a ψ angle in this region of the conformational map. On the contrary, all (βPh)Pro residues adopt ψ values about 10° inferior to those exhibited by L-Pro in the reference compounds ($\psi \approx 140°$) and therefore closer to those considered optimal for βII-folding. As for the *i*+2 residue, significant deviations are observed with respect to the (ϕ,ψ) values of (80,0) in an ideal βII-turn, and the distortion is more pronounced for L-Phe than for D-Phe (Table 1). The latter has been shown to be a general trend when comparing the crystal molecular structures of βII-folded L-Pro-L-Xaa and L-Pro-D-Xaa dipeptides.[10] Indeed, the L-Phe residue in **1** and **3** (as in **5**) is forced to assume positive ϕ values when occupying the *i*+2 position of a βII-turn, that is, to behave as a D residue.

Table 2 Side-chain torsion angles[a] (deg) in the X-ray diffraction structures of dipeptides **1**–**4** and **4a**[b]

			(βPh)Pro–pyrrolidine[c]						(βPh)Pro–phenyl[d]		Phe	
Peptide			θ	χ^1	χ^2	χ^3	χ^4	Puckering	$\chi^{1'}$	$\chi^{2'}$	χ^1	χ^2
Piv-L-*cis*(βPh)Pro-L-Phe-NHMe	**1**		–9	30	–40	34	–16	C^γ-*endo*/C^β-*exo*	157	70/–111	–77	–6/174
Piv-L-*cis*(βPh)Pro-D-Phe-NHMe	**2**		–12	31	–39	31	–12	C^γ-*endo*/C^β-*exo*	160	78/–101	61	56/–126
Piv-L-*trans*(βPh)Pro-L-Phe-NHMe	**3**	mol. A	8	–31	43	–38	18	C^γ-*exo*/C^β-*endo*	–158	73/–109	–90	94/–88
		mol. B	9	–31	43	–37	18	C^γ-*exo*/C^β-*endo*	–157	31/–152	–74	90/–94
Piv-L-*trans*(βPh)Pro-D-Phe-NHMe	**4**	mol. A	11	–34	44	–37	16	C^γ-*exo*/C^β-*endo*	–164	95/–81	72	73/–109
		mol. B	0	19	–32	31	–19	C^γ-*endo*	–107	82/–99	61	100/–82
Boc-L-*trans*(βPh)Pro-D-Phe-NHMe	**4a**	mol. A	8	–28	39	–33	16	C^γ-*exo*/C^β-*endo*	–156	24/–158	57	26/–156
		mol. B	2	–23	35	–33	19	C^γ-*exo*[e]	–151	113/–65	71	33/–154

[a] For standard deviations, see the ESI.‡ [b] The asymmetric unit of **3**, **4** and **4a** contains two independent molecules (A, B). [c] θ (C^δ–N–C^α–C^β dihedral), χ^1, χ^2, χ^3, and χ^4 correspond to the pyrrolidine ring in (βPh)Pro. [d] $\chi^{1'}$ and $\chi^{2'}$ correspond to the phenyl side chain in (βPh)Pro. [e] C^β deviates slightly from the plane leading to some C^β-*endo* character.

View Online

Table 3 Amide NH and C′O stretching frequencies[a] (cm^{-1}) for Piv-L-Pro*-L/D-Phe-NHMe[b] in CH_2Cl_2 solution (c = 5 mM)

Comp.	Peptide sequence	NH(Me)	Phe-NH	Piv-C′O	Pro*-C′O[b]	Phe-C′O
1	L-*cis*(βPh)Pro-L-Phe	3450^{w}/3359^{s}	3436^{m}/3425^{m}/3416^{s}	1620^{vw}/1615^{s}/1604^{w}	1691	1667
3	L-*trans*(βPh)Pro-L-Phe	3448^{w}/3358^{s}	3431^{m}/3412^{s}	1620^{vw}/1614^{s}/1603^{w}	1692^{w}/1686^{s}	1666
5	L-Pro-L-Phe	3448^{w}/3356^{s}	3432^{m}/3414^{s}	1620^{vw}/1612^{s}/1604^{vw}	1684	1666
2	L-*cis*(βPh)Pro-D-Phe	3354	3417	1614^{w}/1602^{s}	1689	1665
4	L-*trans*(βPh)Pro-D-Phe	3349	3414	1614^{w}/1601^{s}	1691	1665
6	L-Pro-D-Phe	3449^{vw}/3345^{s}	3420	1614^{w}/1602^{s}	1691	1665

[a] When the same vibrator gives rise to several absorption bands, their relative intensity is indicated as strong (s), medium (m), weak (w) or very weak (vw). [b] Pro* refers to Pro or the corresponding (βPh)Pro stereoisomer.

Published on 05 October 2011 on http://pubs.rsc.org | doi:10.1039/C1OB06561K
Downloaded by Universitaire d'Angers on 08 February 2012

The L-Pro-L-Xaa and L-Pro-D-Xaa dipeptide sequences are known to prefer β-turns of type I and II, respectively, in environments where intermolecular interactions do not play a significant role.[5,10] In the βI-turn, the *i*+2 L-Xaa residue adopts values near (–90,0), more favourable to its L stereochemistry than those corresponding to the βII-turn, (80,0). However, in a βI-folded L-Pro-L-Xaa dipeptide, the L-Xaa N–H bond is oriented towards the side chains of the two adjacent L-residues and is inaccessible to intermolecular hydrogen bonding,[10,13a] whereas in the βII form this N–H bond points in the opposite direction (as in Fig. 3–7) and can interact with the surrounding molecules. This is the reason why most L-Pro-L-Xaa sequences experience a βI-to-βII transition on going from low-polarity solvents to strongly solvating media[10,13] or the solid state.[5,10,13] In comparison, L-Pro-D-Xaa dipeptides are more propitious to βII-folding in all environments.[5,10,13] The observation of a βII-turn in the solid state for all the dipeptides crystallised in this work (**1**–**4**, **4a**), irrespective of their homochiral or heterochiral sequence, follows this trend. As expected, in all cases, the NH of the L/D-Phe residue is engaged in an intermolecular hydrogen bond with the carbonyl group of a neighbouring molecule. The acceptor site is (βPh)Pro-C′O in compounds **3** and **4**, and Phe-C′O in **1**, **2**, and **4a**.[14]

In solution, the conformation adopted by compounds **1**–**4** was investigated by FT-IR and ^{1}H-NMR spectroscopies. Studies were performed in dichloromethane and deuterochloroform, respectively, on 5–10 mM peptide solutions after having confirmed that no aggregation occurred at these concentrations. For comparative purposes, new spectra were also registered for the reference compounds **5** and **6** under identical conditions to those used for the (βPh)Pro derivatives. The pivaloyl group linked to the pyrrolidine nitrogen presents a two-fold advantage for solution-phase studies: it prevents the *cis* state of the acyl-proline bond for steric reasons and shifts the Piv-C′O frequency out of the IR region typical for peptide carbonyls, thus enabling easier interpretation of spectra.

The IR and NMR studies confirmed that compounds **1**–**4** mainly or exclusively adopt a β-turn conformation in chlorinated solvents, as previously observed for the L-Pro counterparts **5** and **6**.[10,13] Thus, the terminal NH(Me) and Piv-C′O groups are hydrogen-bonded, as evidenced by their low IR stretching frequencies in comparison with those expected for free groups (about 3450 and 1620 cm^{-1}, respectively),[10,13] and this interaction must be intramolecular because intermolecular contacts are discarded at the concentration used. In all cases, the NH(Me) site gives rise to an intense IR band around 3350 cm^{-1} (Table 3) and its proton resonance is only moderately affected by the addition of DMSO-d_6 (Table 4), suggesting that it is engaged in a hydrogen bond.

Table 4 Chemical shift and solvent sensitivity (ppm) of the amide NH proton resonances for Piv-L-Pro*-L/D-Phe-NHMe[a] (c = 10 mM)

		NH(Me)		Phe-NH	
Comp.	Peptide sequence	$CDCl_3$	$\Delta\delta^b$	$CDCl_3$	$\Delta\delta^b$
1	L-*cis*(βPh)Pro-L-Phe	5.66	1.08	5.55	1.92
3	L-*trans*(βPh)Pro-L-Phe	6.49	1.08	6.12	1.65
5	L-Pro-L-Phe	6.68	0.99	5.87	1.74
2	L-*cis*(βPh)Pro-D-Phe	7.11	0.55	5.17	2.85
4	L-*trans*(βPh)Pro-D-Phe	7.56	0.44	5.42	3.02
6	L-Pro-D-Phe	7.33	0.56	5.93	2.33

[a] Pro* refers to Pro or the corresponding (βPh)Pro stereoisomer. [b] Shift of the NH proton resonance on going from $CDCl_3$ to DMSO-d_6 solution.

In comparison, the Phe-NH stretching absorption appears above 3400 cm^{-1} (Table 3) and its proton chemical shift shows a higher sensitivity to DMSO-d_6 solvation (Table 4), as expected for a free NH amide moiety.

In spite of this common behaviour small, yet significant, differences are observed between the homochiral and heterochiral sequences. Thus, the L-L dipeptides **1**, **3** and **5** present a weak absorption near 3450 cm^{-1} (Table 3) that corresponds to a free NH(Me) site and denotes the presence of a small percentage of molecules exhibiting an open conformation devoid of intramolecular hydrogen bonds. This band also appears in the L-Pro-D-Phe derivative (**6**), although with a lower intensity, and cannot be distinguished in the IR spectra of **2** and **4** (Table 3). This suggests that the higher β-turn forming tendency exhibited by the L-Pro-D-Phe sequence in comparison to L-Pro-L-Phe[10,13] (in general, L-Pro-D-Xaa *vs.* L-Pro-L-Xaa dipeptides[10]) is not only maintained but even increased when the natural Pro residue is replaced by (βPh)Pro independently of the *trans* or *cis* stereochemistry of the β-phenyl substituent. The existence of a superior percentage of open conformers in the homochiral peptides is in agreement with the larger variation induced by DMSO-d_6 on their NH(Me) amide proton resonance ($\Delta\delta \approx$ 1.0 and 0.5 ppm for the L-L and L-D dipeptides, respectively; Table 4).

However, the main difference observed in solution does not concern the extent to which the homochiral and heterochiral dipeptides under study adopt a β-turn conformation but the type of β-turn accommodated, which can be unambiguously distinguished by the IR frequency of the Piv-C′O group.[13] The three L-D dipeptides (**2**, **4**, **6**) present an identical profile in this region of the IR spectrum, with a major contribution at 1602 cm^{-1} and a weak absorption near 1612 cm^{-1} (Table 3), which have

 This journal is © The Royal Society of Chemistry 2012

View Online

Published on 05 October 2011 on http://pubs.rsc.org | doi:10.1039/C1OB06561K
Downloaded by Universitaire d'Angers on 08 February 2012

been shown to reflect two different hydrogen-bonded states of the Piv-C′O group in Piv-L-Pro-Xaa-NHR dipeptides, namely those corresponding to a βII- and a βI-turn, respectively.[13] Thus, the βII-turn observed in the solid state for **2** and **4** is also preferred in solution, indicating that the incorporation of a β-phenyl group into L-Pro does not alter the behaviour typically observed for L-Pro-D-Xaa sequences.

In comparison, the L-Pro-L-Phe derivative (**5**) shows two very weak contributions at about 1620 and 1602 cm^{-1}, corresponding, respectively, to a free and a βII-hydrogen-bonded Piv-C′O group, and an intense absorption at 1612 cm^{-1} (Table 3). This indicates the predominance of the βI-turn for **5** in chlorinated solvents, as already established.[10,13] The band near 1602 cm^{-1} becomes slightly more intense in the analogous sequence incorporating L-*cis*(βPh)Pro (**1**) and even more in the L-*trans*(βPh)Pro derivative (**3**) (Table 3), which shows the highest percentage of βII-folded molecules among the three homochiral dipeptides investigated. Yet, the βI-turn remains the preferred conformation for all three compounds in chlorinated solvents.

In the discussion above, the conformation adopted by the peptide backbone in the (βPh)Pro derivatives under study has been considered both in solution and in the solid state. The phenyl substituent attached to the pyrrolidine moiety has been shown not to perturb the conformational properties of L-Pro and, indeed, the β-turn forming propensities of (βPh)Pro resemble closely those of the parent amino acid. However, the arrangement of the side-chain moieties in the compounds investigated and their possible influence on the subtle conformational changes observed upon replacement of L-Pro by *cis* or *trans* L-(βPh)Pro have not been considered yet. They are discussed in the following.

In the crystal, the side chain of the L-Phe residue in dipeptides **1** and **3** (Table 2) exhibits a *gauche*(−) orientation (χ^1 = −74° to −90°) while that of D-Phe in **2**, **4** and **4a** corresponds to *gauche*(+) (χ^1 = 57° to 72°), as respectively found for the parent peptides **5** (χ^1 = −42°)[10] and **6** (χ^1 = 74°).[12] It should be noted that *gauche*(−) is a sterically favoured χ^1 disposition (rotational state of the C^{α}–C^{β} bond) for the L-Phe side chain and is, indeed, the one most commonly encountered in crystallised peptides and proteins.[15] A similar situation corresponds to the *gauche*(+) conformation for D-Phe.

The most remarkable feature in Table 2 regarding χ^1 for the *i*+2 residue (L/D-Phe) is the significantly more negative values attained by this dihedral angle when L-Phe is attached to L-(βPh)Pro, either *cis* (**1**) or *trans* (**3**), in relation to L-Pro (**5**). Actually, the χ^1 angle of L-Phe deviates from the standard value corresponding to a canonical *gauche*(−) orientation (−60°) in opposite directions in **1** and **3** with reference to **5**. In the latter compound, χ^1 = −42° makes the phenyl ring of L-Phe approach the contiguous NH group probably to allow a weak attractive NH···π interaction. In the (βPh)Pro derivatives **1** and **3**, the L-Phe χ^1 moves in the opposite direction (χ^1 ranges from −74° to −90°) and this distinct orientation may be attributed to the interaction established between the two aromatic rings in the (βPh)Pro-containing compounds, which are seen to adopt a parallel arrangement in the *cis* derivative (**1**, Fig. 3) and to be almost perpendicular in both independent molecules of the *trans* compound (**3**, Fig. 5). When D-Phe is present (**2**, **4**, **4a**), the adequate geometry for the two phenyl rings to interact is attained without the need for a significant deviation of χ^1 from the standard 60° value (in molecule B of **4**, it is precluded by the arrangement of the pyrrolidine moiety). The optimisation of such intramolecular aromatic–aromatic interactions also seems to be the basis of the uncommon χ^2 values observed for the L/D-Phe residue in some of the crystallised molecules (Table 2). The χ^2 angle (C^{β}–C^{γ} torsion) reflects the orientation of the phenyl plane with respect to the peptide backbone and is known to prefer values near 90/−90°, for which steric repulsions with the main chain are minimal, with deviations within ±30° being frequent.[15] One notes, however, that some of the χ^2 values assumed by the L/D-Phe residue in the (βPh)Pro-containing dipeptides in Table 2 are severely distorted from this optimal position, as is the case of **4a** (χ^2 = 26/−156° and 33/−154° in molecules A and B, respectively) and, particularly, of **1** (χ^2 = −6/174°). In comparison, the corresponding χ^2 values in the reference compounds **5** and **6** are −68/110° and 63/−122°, respectively. In fact, the variety of orientations adopted by the phenyl plane of the L/D-Phe residue in **1**–**4** and **4a**, reflected in χ^2 (Table 2), seem to be the consequence of the interaction established with the β-phenyl substituent in (βPh)Pro.

The intramolecular aromatic–aromatic interactions observed in the solid state for all the (βPh)Pro derivatives crystallised (with the exception of one of the independent molecules in **4**) seem to be retained in solution only for the sequences incorporating D-Phe, as inferred from the following observations. A striking feature in the ^{1}H-NMR spectra of compounds **2** and **4** in $CDCl_3$, which is also present for the Boc precursors **2a** and **4a**,[14] is the appearance of an aromatic proton near 6.70 ppm. This signal has been assigned to the *ortho* hydrogens of the D-Phe residue. In comparison, all the aromatic protons in the parent D-Phe derivative **6**, that lacks the phenyl ring in the *i*+1 position, appear above 7.10 ppm, as do those in the three L-Phe-containing peptides (**1**, **3**, **5**). The strongly upfield shifted aromatic proton resonance of **2** and **4** can be attributed to the proximity of the phenyl group of the contiguous (βPh)Pro residue. The relative orientation of the two aromatic rings is to be perpendicular, with an *ortho* D-Phe hydrogen pointing to the centre of the phenyl unit in (βPh)Pro.

Such a relative disposition between the two aromatic rings in **2** and **4** differs from that observed in the solid state (Fig. 4 and 6). Molecular models show that it can be achieved if the aromatic moiety of (βPh)Pro is roughly kept as in their respective crystalline structures (in the case of **4**, that in molecule A) while the C^{α}–C^{β} bond of D-Phe is rotated by about 120° (from $\chi^1 \approx 60°$ in the crystals to ≈ −60°) and the phenyl plane is allowed to assume the usual[15] χ^2 values ≈ 90/−90° (±30). Fig. 8 illustrates the relative arrangement of the two aromatic rings when the orientation of the D-Phe side chain in the crystalline structure of **4** (molecule A) is changed in this way.

The modification proposed above for the orientation of the D-Phe side chain in **2** and **4** with respect to that observed in the X-ray diffraction structures is by no means surprising. Actually, it has been proposed to occur for the parent compound containing D-Phe (**6**) on going from the solid state to $CDCl_3$ solution.[10] As previously established and commented above, dipeptide **6** shows a preference for the same βII-turn conformation in both environments. However, the aromatic side chain changes from the *gauche*(+) disposition in the crystal[12] (χ^1 = 74°) to a predominant *gauche*(−) arrangement ($\chi^1 \approx -60°$) in $CDCl_3$ or CH_2Cl_2.[10] The latter places the phenyl ring in the least sterically favoured among the three staggered positions available to χ^1, namely flanked by

Published on 05 October 2011 on http://pubs.rsc.org | doi:10.1039/C1OB06561K
Downloaded by Universitaire d'Angers on 08 February 2012

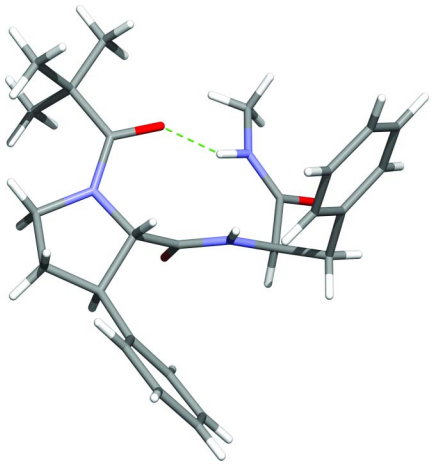

Fig. 8 Molecular model of **4** showing an *ortho* aromatic proton of D-Phe pointing to the centre of the phenyl ring in L-*trans*(βPh)Pro. It has been built from the X-ray diffraction structure of **4** (molecule A) by changing the D-Phe χ^1 torsion from 72° to ≈ –60° and keeping χ^2 in the sterically favourable region ≈ 90/–90° (±30°).

the NH and CO substituents, but provides the optimal geometry for an attractive interaction with the adjacent NH moiety. The existence of this NH···π interaction is reflected[10,13] in the lower IR frequency observed for this NH in **6** (3420 cm^{-1}; Table 3) with respect to the analogous compound incorporating D-Ala in place of D-Phe, in which no aromatic-NH interaction can occur (3430 cm^{-1}).[10] In the crystal, the D-Phe NH moiety is involved in a hydrogen bond with a carbonyl group of a neighbouring molecule[12] and the benzyl side chain adopts the sterically more favourable *gauche*(+) arrangement.

It is highly probable that the D-Phe side chain in **2** and **4** experiences a similar rotation about the C^α–C^β bond on going from the solid state to chlorinated solvents. In fact, the stretching frequency of the D-Phe-NH site in these compounds also indicates the existence of an NH···π interaction (3417 cm^{-1} in **2** and 3414 cm^{-1} in **4**; Table 3) and, therefore, of a high population of the D-Phe χ^1 conformer providing the optimal geometry for it, *gauche*(–). As shown in Fig. 8 for **4**, this arrangement of the D-Phe side chain places an *ortho* hydrogen of this residue pointing to the centre of the phenyl ring in (βPh)Pro, thereby accounting for the upfield aromatic signal observed in the ^{1}H-NMR spectra of **2** and **4**. The population of the *gauche*(–) D-Phe rotamer in **6** was estimated[10,16] to be 52%[17] from the vicinal coupling constants between the α and two β protons measured for this residue in $CDCl_3$ solution. Notably enough, the same method[16] provides an increased percentage of this χ^1 conformer for both **2** (74%) and **4** (66%). The stabilizing interaction established between the two aromatic rings in the latter compounds could contribute to increase the population of *gauche*(–) conformer for D-Phe in spite of being the most sterically hindered staggered arrangement available to χ^1, thus operating in the same sense as does the NH···π interaction. The disappearance of the small amount of open conformers detected for **6** upon replacement of L-Pro by *cis* or *trans* L-(βPh)Pro (to yield **2** and **4**, respectively) could also be related to this additional stabilising interaction. Actually, interactions between the side chain groups of aromatic residues have been recognized as an important stabilizing factor in the conformation of peptides and proteins.[18]

The situation is different for the three L-Phe-containing peptides (**1**, **3**, **5**). There is no evidence that the aromatic contacts observed in the X-ray diffraction structures of **1** and **3** (Fig. 3 and 5) are kept in solution. The orientation of the benzyl side chain of L-Phe in **5** has been shown to change from *gauche*(–) in the crystal[10] (χ^1 = –42°) to a preferential *gauche*(+) arrangement ($\chi^1 \approx 60°$) in $CDCl_3$ solution,[10] thereby bringing the NH and phenyl moieties of L-Phe into close proximity, in an analogous way to that described above for **6** [note that *gauche*(+) for L-Phe is equivalent to *gauche*(–) for D-Phe]. The same modification seems to occur for **1** and **3**, as reflected by the L-Phe-NH stretching frequency that denotes the existence of a similar NH···π interaction in the three homochiral peptides (Table 3). However, it should be noted that in the L-L sequences, this side chain rotation is associated with the βII-to-βI transition experienced by the peptide backbone on going from the solid to the solute state and the combination of both changes makes the phenyl ring of L-Phe move far away from the (βPh)Pro side chain, thus precluding the existence of intramolecular aromatic–aromatic interactions. Not surprisingly, the population of L-Phe *gauche*(+) species estimated[10,16] for **5** in chloroform (54%)[17] is not increased in **1** (56%) and **3** (46%). This fact, together with the observation of a similar percentage of non-β-turn-folded species in solution for the three homochiral dipeptides, suggests that no additional stabilising interaction operates in **1** and **3** with respect to **5**. Obviously, this applies to the major conformer in solution, but does not discard the existence of minor species with a βII-folded backbone in which the L-Phe side chain retains the *gauche*(–) arrangement and interacts with the (βPh)Pro aromatic substituent as in the crystal structures.

The postulated interaction between the two aromatic rings in the D-Phe derivatives **2** and **4** in solution also requires an adequate orientation of the phenyl group in the contiguous (βPh)Pro residue, which should be similar in both compounds and is proposed not to differ much from that observed in the X-ray structures (molecule A for **4**). Such an orientation is given by the *cis*/*trans* stereochemistry at the β carbon and the puckering of the pyrrolidine moiety, as discussed below.

The five-membered ring in all (βPh)Pro derivatives crystallised (Table 2) assumes a puckered conformation, with the γ carbon deviating from the plane towards the same (C^γ-*endo* or down) or the opposite (C^γ-*exo* or up) side of the ring to where the carbonyl group lies.[19] In most of the cases, also the β carbon protrudes from the plane, in the opposite direction to C^γ, so that the conformation is twist (half-chair) instead of envelope-like. The twisted character is highly marked, as indicated by the magnitude of the θ angle (C^δ–N–C^α–C^β dihedral) (Table 2), which gives the extent to which C^β deviates from the plane defined by the atoms involved in the peptide bond (C^δ, N, C^α) and is 0° for an ideal envelope with C^γ at the flap. The frequent occurrence of twist conformations in Table 2 and the strong out-of-plane displacement observed for C^β in them are certainly related to the β-substituted character of (βPh)Pro. Deviation of C^β from planarity alleviates the steric hindrance introduced by the bulky aromatic ring attached to it, which is particularly severe in the *cis* derivative.

In the crystalline state, the two compounds incorporating L-*cis*(βPh)Pro (**1**, **2**) exhibit the same C^γ-*endo*/C^β-*exo* puckering, characterized by positive χ^1 and negative θ values (Table 2; note

 This journal is © The Royal Society of Chemistry 2012

Published on 05 October 2011 on http://pubs.rsc.org | doi:10.1039/C1OB06561K
Downloaded by Universitaire d'Angers on 08 February 2012

that the χ^n values given for (βPh)Pro correspond to the pyrrolidine moiety while those describing the orientation of the phenyl side chain in this residue are termed $\chi^{1'}$ and $\chi^{2'}$). This arrangement moves the β-phenyl ring away from the vicinal carbonyl substituent (Fig. 9a), which would otherwise be eclipsed. Thus, the C′–C$^\alpha$–C$^\beta$–C$_{ipso}$ torsion angle, λ [C′ is the carbonyl carbon and C$_{ipso}$ is the substituted aromatic carbon in (βPh)Pro], is as much as 40° in **1** and 43° in **2**.[14] In this C$^\gamma$-*endo*/C$^\beta$-*exo* half-chair, the phenyl substituent occupies an equatorial position, which is known to minimize steric repulsions with the five-membered ring. The other possible twist arrangement (C$^\gamma$-*exo*/C$^\beta$-*endo*) (Fig. 9b) does not seem to introduce any advantage because the phenyl ring would separate from the contiguous carbonyl substituent in a similar extent (although in the opposite direction, $\lambda \approx -40°$) but would be oriented axially, thus producing severe steric hindrance with some pyrrolidine protons. The latter disposition should then be strongly disfavoured. The five-membered ring in L-*cis*(βPh)Pro is not likely to adopt a C$^\gamma$-envelope conformation either, since keeping C$^\beta$ in the plane would make the β-phenyl and α-carbonyl substituents lie closer to the eclipsed disposition associated with their *cis* stereochemistry.

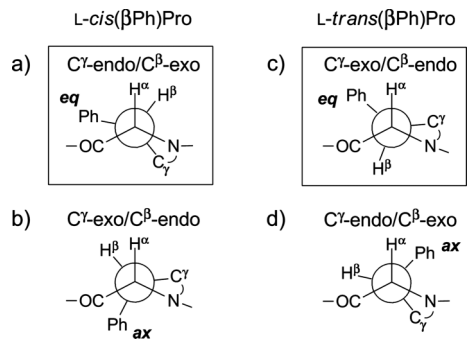

Fig. 9 Newman projection through the C$^\alpha$–C$^\beta$ bond for the two possible half-chair conformations of the pyrrolidine ring in L-*cis*(βPh)Pro (a,b) and L-*trans*(βPh)Pro (c,d). Those observed in the X-ray structures of the *cis* (**1**, **2**) and *trans* peptides (**3**, **4**, **4a**) are marked. The equatorial (*eq*) or axial (*ax*) orientation of the phenyl substituent is indicated.

The C$^\gamma$-*endo*/C$^\beta$-*exo* arrangement observed in the solid state seems therefore to be the most favourable puckering mode of L-*cis*(βPh)Pro. There is strong evidence that this conformation also predominates in solution. The vicinal coupling constants between the pyrrolidine β hydrogen and those in the α ($J_{H\alpha-H\beta} \approx 8.5$ Hz) and γ ($J_{H\beta-H\gamma endo} \approx 13$ Hz, $J_{H\beta-H\gamma exo} \approx 6$ Hz) positions[20] measured in $CDCl_3$ are similar for **1** and **2** (Table 5) and are in excellent agreement with those calculated from their X-ray diffraction geometries (Table 5). The latter have been estimated[21,22] using the modification of the Karplus equation developed by Haasnoot *et al.*, which has been shown to provide more reliable estimates for the proline system.[23] In contrast, a very small $J_{H\beta-H\gamma endo}$ value (<2 Hz) is expected for the other possible half-chair arrangement (C$^\gamma$-*exo*/C$^\beta$-*endo*) (Table 5). The large $J_{H\beta-H\gamma endo}$ measured for both **1** and **2** allows us to discard the presence of a significant population of species exhibiting the latter pyrrolidine shape. Another argument supporting the assignment of a highly predominant C$^\gamma$-*endo*/C$^\beta$-*exo* conformation for L-*cis*(βPh)Pro in solution is the observation in **1** and **2** (shown in Fig. 10 for **1**) of a NOE cross-peak between H$^\beta$ and H$^\delta_{exo}$, denoting their proximity, along with the absence of

Table 5 Comparison of the vicinal coupling constants (Hz) of the β hydrogen of L-*cis*(βPh)Pro measured in **1** and **2** with those estimated for different arrangements of the pyrrolidine ring

	Calculated[b]		Observed[c]	
$^3J_{H-H}$[a]	C$^\gamma$-*endo*/ C$^\beta$-*exo*[d,e]	C$^\gamma$-*exo*/ C$^\beta$-*endo*[d]	**1**	**2**
H$^\alpha$–H$^\beta$	7.5	6.4	8.6	8.3
H$^\beta$–H$^\gamma_{endo}$	12.5	1.5	11.9	13.9
H$^\beta$–H$^\gamma_{exo}$	5.7	4.4	6.1	6.0

[a] The pyrrolidine γ hydrogens are labelled as *endo* or *exo* as indicated in note 20. [b] Using the Haasnoot–Altona equation (ref. 21,22). [c] $CDCl_3$ solution. [d] Half-chair (twist) conformation. [e] Estimated from the geometry observed in the crystalline structure of **1** (similar results are obtained from that of **2**).

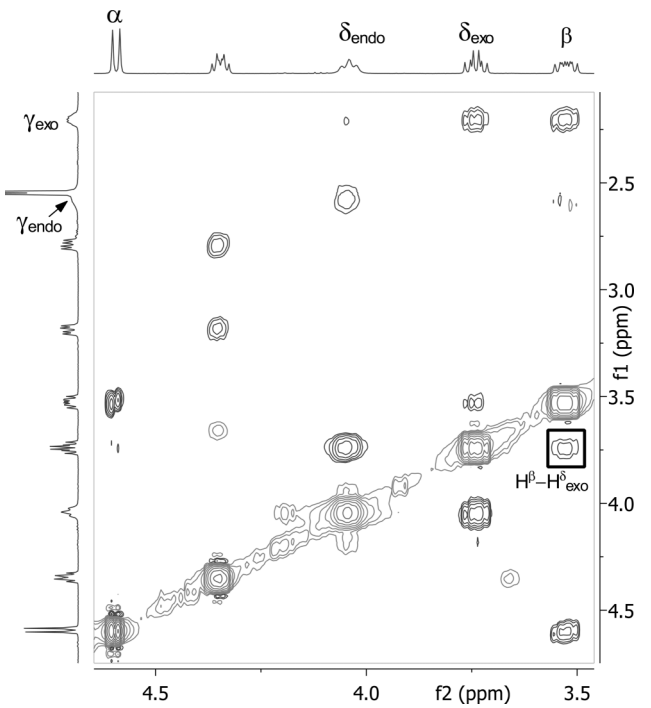

Fig. 10 Section of the NOESY spectrum of compound **1** in $CDCl_3$ solution (10 mM), showing the pyrrolidine H$^\beta$–H$^\delta_{exo}$ cross-peak. The absence of H$^\alpha$–H$^\gamma_{exo}$ correlation is also noteworthy. The hydrogen atoms labelled[20] correspond to the (βPh)Pro residue.

correlation between H$^\alpha$ and H$^\gamma_{exo}$. The two latter protons should become close for a γ carbon deviating in the opposite direction to the carbonyl substituent (C$^\gamma$-*exo*), that is, towards the α hydrogen (Fig. 9b).

The situation for the *trans* isomer is more complex. In most of the crystallised molecules, the five-membered ring of L-*trans*(βPh)Pro adopts a half-chair conformation (Table 2). Displacement of the β carbon occurs in the direction that places the phenyl substituent in an equatorial position (C$^\beta$-*endo*), with θ values around 10°, and the γ carbon moves towards the opposite side (C$^\gamma$-*exo*). However, this C$^\gamma$-*exo*/C$^\beta$-*endo* arrangement (Fig. 9c) makes the phenyl and carbonyl substituents approach (note that they are *trans* here), with λ angles about 80° being observed in the X-ray structures.[14] Accordingly, deviation of C$^\beta$ from the plane to place the aromatic ring equatorially is not as advantageous as

Published on 05 October 2011 on http://pubs.rsc.org | doi:10.1039/C1OB06561K
Downloaded by Universitaire d'Angers on 08 February 2012

seen before for the *cis* isomer, in which case it also provided the maximum separation between the vicinal substituents.

This probably explains why other pyrrolidine arrangements other than the most abundant C$^{\gamma}$-*exo*/C$^{\beta}$-*endo* half-chair are seen among the crystallised *trans*(βPh)Pro-containing peptides (Table 2). Thus, molecule B of **4a** retains the C$^{\gamma}$-*exo* disposition found for most *trans* compounds but C$^{\beta}$ remains near the ring plane (θ = 2°) so that the puckering is close to a C$^{\gamma}$-*exo* envelope. As a result, the phenyl substituent is pseudoequatorial (an intermediate position between that corresponding to a planar ring and the equatorial one in a half-chair), but this less favourable orientation is somehow compensated for by the lower proximity to the carbonyl substituent (λ = 90°).[14] It appears, therefore, that conformations with a geometry intermediate between a C$^{\gamma}$-*exo*/C$^{\beta}$-*endo* half-chair and a C$^{\gamma}$-*exo* envelope are also accessible to L-*trans*(βPh)Pro, although they are expected to be less stable than the half-chair.

Additionally, a third type of pyrrolidine puckering is seen among the X-ray structures of the *trans*(βPh)Pro derivatives, namely that in molecule B of **4** (Table 2). In this case, C$^{\beta}$ lies in the plane formed by the atoms involved in the peptide bond (θ = 0°) and a pure C$^{\gamma}$-*endo* envelope is seen. This arrangement provides the maximum distance with the carbonyl moiety (λ = 134°)[14] while making the aromatic substituent pseudoaxial.

The other possible half-chair of L-*trans*(βPh)Pro (C$^{\gamma}$-*endo*/C$^{\beta}$-*exo*) is not observed in any of the compounds crystallised. It would introduce the maximum distance between the α and β substituents ($\lambda \approx 150°$, Fig. 9d) but also orientate the phenyl substituent axially and therefore introduce severe steric repulsions. Indeed, when C$^{\gamma}$ is *endo*, there seems to be no benefit in C$^{\beta}$ also deviating from the plane, that is, in changing from the C$^{\gamma}$-*endo* envelope observed in the molecule B of **4** to the C$^{\gamma}$-*endo*/C$^{\beta}$-*exo* half-chair, since λ is slightly superior ($\Delta\lambda \approx 15°$) but at the cost of increasing the axial character of the aromatic substituent. Accordingly, the C$^{\gamma}$-*endo* envelope but not the C$^{\gamma}$-*endo*/C$^{\beta}$-*exo* twist form is seen among the *trans* compounds crystallised. Yet, the stability difference between the two half-chairs in *trans*(βPh)Pro is expected to be less marked than in the *cis* derivative because, in the latter, the most stable half-chair combines an equatorial phenyl group and the maximum possible separation between the bulky vicinal substituents whereas this is not the case for the *trans* compound.

The vicinal coupling constants measured for the L-*trans*(βPh)Pro H$^{\beta}$ in $CDCl_3$ solution for **3** and **4** are substantially different (Table 6), indicating that the pyrrolidine puckering differs in the two compounds. Comparison of the experimental values with those predicted[21,22] for the different geometries exhibited by the five-membered ring in the crystalline structures of the *trans* compounds (Table 6) suggests that dipeptide **4** adopts with high preference a C$^{\gamma}$-*exo* arrangement. Whether it corresponds to a C$^{\gamma}$-*exo*/C$^{\beta}$-*endo* half-chair, a C$^{\gamma}$-*exo* envelope, a mixture of both or a single conformation with an intermediate geometry is difficult to ascertain on the basis of the *J* values only. However, the greater stability expected for the half-chair form, which correlates with its more frequent occurrence in the X-ray structures, together with the detection[14] of NOE cross-peaks between H$^{\beta}$ and H$^{\delta}_{endo}$ (that get close for an *endo* C$^{\beta}$) and the H$^{\alpha}$–H$^{\gamma}_{exo}$ protons (denoting the *exo* arrangement of C$^{\gamma}$) point to a situation proximal to the C$^{\gamma}$-*exo*/C$^{\beta}$-*endo* half-chair, as observed in the crystalline state for most L-*trans*(βPh)Pro derivatives (Table 2). In any case, and most importantly, the large magnitude of $J_{H\alpha-H\beta}$ (9.3 Hz) and $J_{H\beta-H\gamma exo}$ (11.8 Hz) measured for this compound allows us to discard the presence of a significant ratio of C$^{\gamma}$-*endo* conformers, for which very small $J_{H\alpha-H\beta}$ (0.6–2.1 Hz) and $J_{H\beta-H\gamma exo}$ (<1 Hz) values are expected (Table 6). Conversely, the coupling constants observed for H$^{\beta}$ in **3** can only be explained if a non-negligible population of C$^{\gamma}$-*endo*-puckered species is present (40–60%). In such conformers, an *ortho* proton of the (pseudo)axial phenyl ring becomes close to H$^{\delta}_{exo}$ and, accordingly, a NOE cross-peak appears.[14] This fact together with the NOE correlation detected between H$^{\alpha}$ and H$^{\gamma}_{exo}$, typical of the C$^{\gamma}$-*exo* arrangement, is consistent with the coexistence of C$^{\gamma}$-*endo* and C$^{\gamma}$-*exo* shapes in **3**. Again, it is difficult to discern from these results the extent to which they are envelope-like or twist, that is, the degree of non-planarity at C$^{\beta}$. Yet, they are most probably of the C$^{\gamma}$-*endo* envelope and C$^{\gamma}$-*exo*/C$^{\beta}$-*endo* half-chair types, respectively, according to the X-ray diffraction results and the comments thereof. It is worth noting that the higher flexibility observed for the pyrrolidine ring in *trans*(βPh)Pro with respect to the *cis* isomer is in agreement with the results from computational analysis on diamide derivatives of the β-isopropyl counterparts.[24]

Table 6 Comparison of the vicinal coupling constants (Hz) of the β hydrogen of L-*trans*(βPh)Pro measured in **3** and **4** with those estimated for different arrangements of the pyrrolidine ring

	Calculated[b]				Observed[c]	
$^3J_{H-H}$[a]	C$^{\gamma}$-*exo*/ C$^{\beta}$-*endo*[d,e]	C$^{\gamma}$-*exo*[f,g]	C$^{\gamma}$-*endo*[f,h]	C$^{\gamma}$-*endo*/ C$^{\beta}$-*exo*[d]	**3**	**4**
H$^{\alpha}$–H$^{\beta}$	11.1	9.9	2.1	0.6	5.5	9.3
H$^{\beta}$–H$^{\gamma}_{endo}$	5.1	6.8	9.3	5.6	≈ 6.5[i]	6.3
H$^{\beta}$–H$^{\gamma}_{exo}$	12.7	11.9	0.5	1.0	≈ 7.5[i]	11.8

[a] The pyrrolidine γ hydrogens are labelled as *endo* or *exo* as indicated in note 20. [b] Using the Haasnoot–Altona equation (ref. 21,22). [c] $CDCl_3$ solution. [d] Half-chair (twist) conformation. [e] Estimated from the geometry observed in the crystalline structure of mol. A of **3**. [f] Envelope or envelope-like conformation. [g] Estimated from the geometry observed in the crystalline structure of mol. B of **4a** (there is some C$^{\beta}$-*endo* character, see Table 2). [h] Estimated from the geometry observed in the crystalline structure of mol. B of **4**. [i] Not determined with higher precision due to signal overlapping.

According to the above discussion, the pyrrolidine ring in the *cis* derivative **2** and the *trans* compound **4** adopts in solution a conformation close to that observed in the solid state for each compound (molecule A in the latter case). It is interesting to note that the proposed intramolecular interaction between the aromatic moieties in these peptides is based on an orientation of the phenyl ring in (βPh)Pro similar to those in the crystals (molecule A for **4**). Even if the β-phenyl substituent is *cis* in **2** and *trans* in **4**, their respective C$^{\gamma}$-*endo*/C$^{\beta}$-*exo* and C$^{\gamma}$-*exo*/C$^{\beta}$-*endo* arrangements, observed in the solid state and believed to be highly predominant in solution, place this group in positions that are much closer than *a priori* expected from their different stereochemistry (compare Fig. 9a and 9c). Thus, the $\chi^{1'}$ values in Table 2, giving the orientation of the phenyl substituent in (βPh)Pro with respect to the peptide backbone (N–C$^{\alpha}$–C$^{\beta}$–C$_{ipso}$), are of 160° in **2** and –164° in **4** (molecule A), which means a difference of only 36°. When the relative orientation of the aromatic substituent is compared taking as a reference the position of the carbonyl group, a similar result is obtained: λ is 43° in **2** and 75° in **4** (molecule A).[14] Therefore, the (βPh)Pro aromatic group

 This journal is © The Royal Society of Chemistry 2012

Published on 05 October 2011 on http://pubs.rsc.org | doi:10.1039/C1OB06561K
Downloaded by Universitaire d'Angers on 08 February 2012

in **2** and **4** are not so differently oriented in solution, and this is consistent with the existence, in both cases, of a similar interaction with the D-Phe residue exhibiting the same *gauche*(−) side-chain arrangement. In each case, small χ^1/χ^2 variations in the latter residue could allow for the optimal geometry. In turn, the fact that this orientation of the (βPh)Pro phenyl group in **4** is necessary for this interaction to occur could be the reason why the C^{γ}-*exo*/C^{β}-*endo* pyrrolidine conformation is overwhelmingly populated in solution for this compound whereas the same does not hold true for **3**. In other words, the existence of an interaction with the aromatic ring of D-Phe could shift the conformational equilibrium of the pyrrolidine ring in **4** towards the puckering mode providing the adequate geometry for it. In **3**, the presence of L-Phe instead of D-Phe does not allow for this interaction to occur and, accordingly, such equilibrium is not shifted to any particular conformer.

Conclusions

The structural propensities of homochiral and heterochiral dipeptide sequences that incorporate in the *i*+1 position the L-Pro analogues L-*cis*(βPh)Pro and L-*trans*(βPh)Pro have been determined in solution and the solid state and compared to those induced by the natural amino acid. The phenyl substituent attached to the pyrrolidine β carbon has been shown to be fully compatible with the conformational properties of L-Pro and, thus, (βPh)Pro essentially retains the β-turn forming propensities of the parent amino acid. In the solid state, all the (βPh)Pro derivatives crystallised adopt a βII-turn, as do the analogous compounds containing L-Pro. In solution, L-*trans*(βPh)Pro induces a higher β-turn folding ratio while the preference for the βI or βII folding modes parallels that of the natural sequences, with only subtle differences.

The pyrrolidine conformation is significantly affected by the presence of the β-phenyl group. The puckering modes that alleviate most the steric hindrance introduced by this substituent are preferred. The *cis*(βPh)Pro residue shows a marked propensity for the C^{γ}-*endo*/C^{β}-*exo* arrangement both in the solid state and in solution whereas the *trans* compound exhibits a higher flexibility, with different pyrrolidine shapes being accessible. As a consequence, the phenyl group in *cis*(βPh)Pro is fixed at χ^1 near 160°, while in *trans*(βPh)Pro it may explore the −160° (for a C^{γ}-*exo*/C^{β}-*endo* pyrrolidine half-chair) or −110° (C^{γ}-*endo* envelope) regions. This issue is essential when a particular spatial arrangement is required for interaction with the receptor binding pocket if (βPh)Pro is inserted into a biologically active peptide or for other applications requiring well-oriented substituents.

Interactions between the aromatic ring of (βPh)Pro and the contiguous L- or D-Phe residue are observed in all the dipeptides crystallised. In solution, they seem to occur only for the heterochiral sequences. This intramolecular aromatic–aromatic interaction may be responsible for the higher β-turn ratio observed for such sequences and may also affect the conformational preferences of the pyrrolidine ring.

Experimental section

General

All reagents were used as received from commercial suppliers without further purification. Enantiomerically pure Boc-L-*cis*(βPh)Pro-OH and Boc-L-*trans*(βPh)Pro-OH were obtained by chromatographic resolution of a racemic precursor; details will be reported elsewhere. Thin-layer chromatography (TLC) was performed on Macherey-Nagel Polygram® SIL G/UV_{254} precoated silica gel polyester plates. The products were visualized by exposure to UV light or submersion in ninhydrin or cerium molybdate stain [aqueous solution of phosphomolybdic acid (2%), $CeSO_4 \cdot 4H_2O$ (1%) and H_2SO_4 (6%)]. Column chromatography was performed using 60 M (0.04–0.063 mm) silica gel from Macherey-Nagel. Melting points were determined on a Gallenkamp apparatus. IR spectra in the solid state were recorded on a Nicolet Avatar 360 FTIR spectrophotometer; ν_{max} is given for the main absorption bands. ^{1}H- and ^{13}C-NMR spectra were registered at room temperature on a Bruker AV-500 or AV-400 instrument, respectively, using the residual solvent signal as the internal standard; chemical shifts (δ) are expressed in ppm and coupling constants (J) in Hertz. Peptide solutions at 10 mM concentration were used for the ^{1}H-NMR spectra. Complete assignment of all proton resonances was performed on the basis of COSY, NOESY (500 ms mixing time), and HSQC experiments registered on the Bruker AV-500 instrument on 10 mM peptide solutions. High-resolution mass spectra were recorded on a Bruker Microtof-Q spectrometer.

General procedure for the synthesis of peptides 1–4

Boc-L-*cis*(βPh)Pro-OH or Boc-L-*trans*(βPh)Pro-OH (500 mg, 1.72 mmol) was suspended in acetonitrile (20 mL) and BOP [(benzotriazol-1-yloxy)tris(dimethylamino)phosphonium hexafluorophosphate] (912 mg, 2.06 mmol) was added. After 10 min, *N*,*N*-diisopropylethylamine (0.66 mL, 3.78 mmol) was added followed by L- or D-Phe-NHMe hydrochloride (552 mg, 2.58 mmol) and the stirring was continued for 4 days. The solvent was evaporated and the remaining residue was redissolved in dichloromethane (30 mL). The solution was successively washed with 5% aqueous potassium bisulfate (15 mL), 5% aqueous sodium bicarbonate (15 mL), and brine (15 mL). The organic layer was dried over anhydrous $MgSO_4$ and filtered. Evaporation of the solvent followed by column chromatography (eluent: ethyl acetate–dichloromethane–hexanes 6 : 3 : 1) furnished the corresponding *N*-Boc protected dipeptide **1a–4a** (644–690 mg, 1.43–1.53 mmol, 83–89% yield; full characterization is given in the ESI‡). A 3N solution of hydrogen chloride in ethyl acetate (5 mL) was then added to **1a–4a** (500 mg, 1.11 mmol) and the suspension formed was stirred at room temperature for 2 h. After evaporation of the solvent, the residue was taken up in water and lyophilized. The resulting solid was suspended in chloroform (10 mL) and *N*-methylmorpholine (0.27 mL, 2.44 mmol) and pivaloyl chloride (0.16 mL, 1.33 mmol) were added. The reaction mixture was stirred at room temperature for 24 h. Evaporation of the solvent followed by column chromatography (eluent: hexanes–ethyl acetate 1 : 9) provided the desired dipeptide **1–4** in the yield indicated in each case.

Piv-L-*cis*(βPh)Pro-L-Phe-NHMe (1). (459 mg, 1.05 mmol, 95% yield); mp 199 °C; $[\alpha]_D^{20}$ = +64.1 (c = 0.40, MeOH); IR (nujol) ν_{max}/cm^{-1} 3341, 3306, 1667, 1652, 1604; ^{1}H-NMR (500 MHz, $CDCl_3$, c = 10 mM) δ_H 1.20 (9H, s, Piv), 2.21 (1H, m, Pro-$H^{\gamma}{}_{exo}$), 2.55 (3H, d, J = 4.5 Hz, NH*Me*) overlapped with 2.47–2.67 (1H, m, Pro-$H^{\gamma}{}_{endo}$), 2.79 (1H, dd, J = 13.8, 6.3 Hz, Phe-H^{β}), 3.19 (1H, dd, J = 13.8, 5.4 Hz, Phe-H^{β}), 3.53 (1H, ddd, J = 11.9, 8.6,

Published on 05 October 2011 on http://pubs.rsc.org | doi:10.1039/C1OB06561K
Downloaded by Universitaire d'Angers on 08 February 2012

6.1 Hz, Pro-H$^{\beta}$), 3.75 (1H, m, Pro-H$^{\delta}_{exo}$), 4.05 (m, 1H, Pro-H$^{\delta}_{endo}$), 4.35 (1H, ddd, J = 8.4, 6.3, 5.4 Hz, Phe-H$^{\alpha}$), 4.60 (1H, d, J = 8.6 Hz, Pro-H$^{\alpha}$), 5.55 (1H, br d, J = 8.4 Hz, Phe-N*H*), 5.66 (1H, m, N*H*Me), 7.10–7.19 (4H, m, Ar), 7.21–7.34 (6H, m, Ar); ^{13}C-NMR (100 MHz, $CDCl_3$) δ_C 26.23 (NHMe), 27.14 (Piv-Me$_3$), 29.91 (Pro-C$^{\gamma}$), 36.84 (Phe-C$^{\beta}$), 39.15 (Piv-C), 44.87 (Pro-C$^{\beta}$), 48.13 (Pro-C$^{\delta}$), 53.35 (Phe-C$^{\alpha}$), 67.51 (Pro-C$^{\alpha}$), 126.93 (Ar), 127.40 (Ar), 127.92 (Ar), 128.47 (Ar), 128.64 (Ar), 129.48 (Ar), 136.76 (Ar), 136.83 (Ar), 169.37 (CO), 170.65 (CO), 177.95 (Piv-CO); HRMS (ESI) $C_{26}H_{33}N_3NaO_3$ [M+Na]$^+$: calcd. 458.2414, found 458.2437.

Piv-L-*cis*(βPh)Pro-D-Phe-NHMe (2). (377 mg, 0.87 mmol, 78% yield); mp 260 °C; $[\alpha]_D^{20}$ = +98.4 (c = 0.34, MeOH); IR (nujol) ν_{max}/cm^{-1} 3330, 3276, 1672, 1653, 1606; ^{1}H-NMR (500 MHz, $CDCl_3$, c = 10 mM) δ_H 1.26 (9H, s, Piv), 2.07 (1H, dd, J = 13.6, 6.0 Hz, Phe-H$^{\beta}$), 2.18 (1H, m, Pro-H$^{\gamma}_{exo}$), 2.68 (3H, d, J = 4.0 Hz, NH*Me*), 2.97 (1H, m, Pro-H$^{\gamma}_{endo}$), 3.33 (1H, dd, J = 13.6, 3.8 Hz, Phe-H$^{\beta}$), 3.47 (1H, ddd, J = 13.9, 8.3, 6.0 Hz, Pro-H$^{\beta}$), 3.72 (1H, m, Pro-H$^{\delta}_{exo}$), 4.16–4.22 (1H, m, Pro-H$^{\delta}_{endo}$) overlapped with 4.20 (1H, d, J = 8.3 Hz, Pro-H$^{\alpha}$), 4.40 (1H, ddd, J = 9.5, 6.0, 3.8 Hz, Phe-H$^{\alpha}$), 5.17 (1H, br d, J = 9.5 Hz, Phe-N*H*), 6.70 (2H, m, Ar), 7.11 (1H, m, N*H*Me), 7.13–7.21 (3H, m, Ar), 7.27–7.46 (5H, m, Ar); ^{13}C-NMR (100 MHz, $CDCl_3$) δ_C 26.37 (NHMe), 27.18 (Piv-Me$_3$), 29.76 (Pro-C$^{\gamma}$), 35.60 (Phe-C$^{\beta}$), 38.87 (Piv-C), 45.49 (Pro-C$^{\beta}$), 48.39 (Pro-C$^{\delta}$), 52.40 (Phe-C$^{\alpha}$), 68.44 (Pro-C$^{\alpha}$), 126.94 (Ar), 127.82 (Ar), 128.21 (Ar), 128.56 (Ar), 128.62 (Ar), 129.50 (Ar), 135.85 (Ar), 136.24 (Ar), 170.11 (CO), 170.73 (CO), 178.15 (Piv-CO); HRMS (ESI) $C_{26}H_{33}N_3NaO_3$ [M+Na]$^+$: calcd. 458.2414, found 458.2393.

Piv-L-*trans*(βPh)Pro-L-Phe-NHMe (3). (343 mg, 0.79 mmol, 71% yield); mp 143 °C; $[\alpha]_D^{25}$ = +53.4 (c = 0.47, MeOH); IR (nujol) ν_{max}/cm^{-1} 3331, 3315, 1671, 1660, 1607; ^{1}H-NMR (500 MHz, $CDCl_3$, c = 10 mM) δ_H 1.17 (9H, s, Piv), 2.03 (1H, m, Pro-H$^{\gamma}_{exo}$), 2.29 (1H, m, Pro-H$^{\gamma}_{endo}$), 2.74 (3H, d, J = 4.6 Hz, NH*Me*), 3.10 (1H, dd, J = 14.0, 6.0 Hz, Phe-H$^{\beta}$), 3.34 (1H, dd, J = 14.0, 6.7 Hz, Phe-H$^{\beta}$), 3.44 (1H, ddd, J = ≈ 7.5, ≈ 6.5, 5.5 Hz, Pro-H$^{\beta}$), 3.60 (1H, m, Pro-H$^{\delta}_{endo}$), 3.89 (1H, m, Pro-H$^{\delta}_{exo}$), 4.53 (1H, d, J = 5.5 Hz, Pro-H$^{\alpha}$), 4.61 (1H, ddd, J = 8.4, 6.7, 6.0 Hz, Phe-H$^{\alpha}$), 6.12 (1H, br d, J = 8.4 Hz, Phe-N*H*), 6.49 (1H, m, N*H*Me), 7.10–7.33 (10H, m, Ar); ^{13}C-NMR (100 MHz, $CDCl_3$) δ_C 26.27 (NHMe), 27.09 (Piv-Me$_3$), 34.01 (Pro-C$^{\gamma}$), 36.72 (Phe-C$^{\beta}$), 39.00 (Piv-C), 45.55 (Pro-C$^{\beta}$), 47.72 (Pro-C$^{\delta}$), 53.94 (Phe-C$^{\alpha}$), 68.77 (Pro-C$^{\alpha}$), 126.83 (Ar), 126.88 (Ar), 127.10 (Ar), 128.60 (Ar), 128.74 (Ar), 129.21 (Ar), 137.02 (Ar), 140.68 (Ar), 170.93 (CO), 170.99 (CO), 178.22 (Piv-CO); HRMS (ESI) $C_{26}H_{33}N_3NaO_3$ [M+Na]$^+$: calcd. 458.2414, found 458.2398.

Piv-L-*trans*(βPh)Pro-D-Phe-NHMe (4). (396 mg, 0.91 mmol, 82% yield); mp 208 °C; $[\alpha]_D^{25}$ = +106.9 (c = 0.46, MeOH); IR (nujol) ν_{max}/cm^{-1} 3332, 3297, 1657, 1623, 1609; ^{1}H-NMR (500 MHz, $CDCl_3$, c = 10 mM) δ_H 1.27 (9H, s, Piv), 2.15 (1H, m, Pro-H$^{\gamma}_{exo}$), 2.37 (1H, m, Pro-H$^{\gamma}_{endo}$), 2.69 (1H, dd, J = 13.8, 5.5 Hz, Phe-H$^{\beta}$), 2.74 (3H, d, J = 4.5 Hz, NH*Me*), 3.37 (1H, dd, J = 13.8, 5.1 Hz, Phe-H$^{\beta}$), 3.41 (1H, ddd, J = 11.8, 9.3, 6.3 Hz, Pro-H$^{\beta}$), 3.81 (1H, m, Pro-H$^{\delta}_{endo}$), 3.93 (1H, d, J = 9.3 Hz, Pro-H$^{\alpha}$), 4.08 (1H, m, Pro-H$^{\delta}_{exo}$), 4.76 (1H, ddd, J = 10.0, 5.5, 5.1 Hz, Phe-H$^{\alpha}$), 5.42 (1H, br d, J = 10.0 Hz, Phe-N*H*), 6.69 (2H, m, Ar), 7.05–7.23 (5H, m, Ar), 7.32–7.42 (3H, m, Ar), 7.56 (1H, m, N*H*Me); ^{13}C-NMR (100 MHz, $CDCl_3$) δ_C 26.46 (NHMe), 27.09 (Piv-Me$_3$), 34.31 (Pro-C$^{\gamma}$), 36.08 (Phe-C$^{\beta}$), 38.75 (Piv-C), 46.78 (Pro-C$^{\beta}$), 49.15 (Pro-C$^{\delta}$), 52.77 (Phe-C$^{\alpha}$), 71.13 (Pro-C$^{\alpha}$), 126.79 (Ar), 127.26 (Ar), 127.57 (Ar), 128.56 (Ar), 128.95 (Ar), 129.29 (Ar), 135.95 (Ar), 139.15 (Ar), 170.94 (CO), 171.31 (CO), 177.65 (Piv-CO); HRMS (ESI) $C_{26}H_{33}N_3NaO_3$ [M+Na]$^+$: calcd. 458.2414, found 458.2396.

IR spectroscopy in solution

IR spectra were recorded in a Nicolet Avatar 360 FTIR spectrophotometer working at a resolution of 2 cm^{-1} and averaging a total of 256 scans. A cell equipped with CaF_2 windows and a path length fixed at 0.5 mm was used. The sample chamber was flushed continuously with dry air. Measurements were carried out at room temperature in dichloromethane at peptide concentrations of 5 mM. The absence of solute–solute interactions was confirmed by the fact that unmodified spectra were obtained after further dilution. Absorbance of samples was calculated by subtracting the pure solvent spectrum scanned under the same conditions. Second-derivative and curve-decomposition of spectra were carried out to obtain the absorption maxima of overlapping bands.

X-ray diffraction structures

Single crystals were obtained by slow evaporation from dichloromethane–ethyl acetate–hexanes (**1**), diethyl ether–ethyl acetate (**2**) or diisopropyl ether–dichloromethane (**3**, **4**, **4a**) solutions. The X-ray diffraction data were collected at 150 K on an Oxford Diffraction Xcalibur diffractometer provided with a Sapphire CCD detector, using graphite monochromated Mo-Kα radiation (λ = 0.71073 Å). The structures were solved by direct methods using SHELXS-97[25a] and refinement was performed using SHELXL-97[25b] by the full-matrix least-squares technique with anisotropic thermal factors for heavy atoms. Hydrogen atoms were located by calculation (except those at the nitrogen atoms, which were found on the *E*-map) and affected by an isotropic thermal factor fixed to 1.2 times the U_{eq} of the carrier atom (1.5 for the methyl protons). CCDC 842881–842885 contain the supplementary crystallographic data for this paper.‡ These data can be obtained free of charge from the Cambridge Crystallographic Data Centre *via* www.ccdc.cam.ac.uk/data_request/cif.

Summary of crystallographic data for **1** ($C_{26}H_{33}N_3O_3$): monoclinic, space group $P2_1$; a = 5.7243(3) Å, b = 18.0071(8) Å, c = 11.1680(5) Å, β = 96.429(4)°; Z = 2; d_{calcd} = 1.265 g cm^{-3}; 11168 reflections collected, 4431 unique (R_{int} = 0.033); data/parameters: 4431/291; final R indices ($I > 2\sigma I$): R_1 = 0.033, wR_2 = 0.056; highest residual electron density: 0.16 e Å^{-3}.

Summary of crystallographic data for **2** ($C_{26}H_{33}N_3O_3$): monoclinic, space group $P2_1$; a = 5.7726(6) Å, b = 17.590(2) Å, c = 11.5824(14) Å, β = 96.205(10)°; Z = 2; d_{calcd} = 1.237 g cm^{-3}; 20298 reflections collected, 4111 unique (R_{int} = 0.104); data/parameters: 4111/290; final R indices ($I > 2\sigma I$): R_1 = 0.048, wR_2 = 0.087; highest residual electron density: 0.21 e Å^{-3}.

Summary of crystallographic data for **3** ($C_{26}H_{33}N_3O_3$): monoclinic, space group $P2_1$; a = 9.5504(3) Å, b = 25.2883(7) Å, c = 10.0653(3) Å, β = 103.733(3)°; Z = 4; d_{calcd} = 1.225 g cm^{-3}; 57501 reflections collected, 10806 unique (R_{int} = 0.044); data/parameters: 10806/579; final R indices ($I > 2\sigma I$): R_1 = 0.031, wR_2 = 0.057; highest residual electron density: 0.14 e Å^{-3}.

This journal is © The Royal Society of Chemistry 2012

Published on 05 October 2011 on http://pubs.rsc.org | doi:10.1039/C1OB06561K
Downloaded by Universitaire d'Angers on 08 February 2012

Summary of crystallographic data for **4** ($C_{26}H_{33}N_3O_3$): monoclinic, space group $P2_1$; a = 9.6700(3) Å, b = 12.4890(5) Å, c = 19.8078(7) Å, β = 93.060(3)°; Z = 4; d_{calcd} = 1.211 g cm^{-3}; 17815 reflections collected, 9060 unique (R_{int} = 0.038); data/parameters: 9060/580; final R indices ($I > 2\sigma I$): R_1 = 0.055, wR_2 = 0.091; highest residual electron density: 0.19 e Å^{-3}.

Summary of crystallographic data for **4a** ($C_{26}H_{33}N_3O_4$): monoclinic, space group $P2_1$; a = 13.539(2) Å, b = 13.615(2) Å, c = 13.6874(17) Å, β = 97.1390(12)°; Z = 4; d_{calcd} = 1.198 g cm^{-3}; 14654 reflections collected, 7271 unique (R_{int} = 0.077); data/parameters: 7271/597; final R indices ($I > 2\sigma I$): R_1 = 0.056, wR_2 = 0.091; highest residual electron density: 0.16 e Å^{-3}.

Acknowledgements

The authors thank the Ministerio de Ciencia e Innovación – FEDER (project CTQ2010-17436; FPU fellowship to P.F.) and Gobierno de Aragón (research group E40) for financial support.

References

1 (*a*) *Peptide and Protein Design for Biopharmaceutical Applications*, ed. K. J. Jensen, John Wiley & Sons, Chichester, 2009; (*b*) *Foldamers: Structure, Properties, and Applications*, ed. S. Hecht and I. Huc, Wiley-VCH, Weinheim, 2007.

2 For reviews, see: (*a*) K. Estieu-Gionnet and G. Guichard, *Expert Opin. Drug Discovery*, 2011, **6**, 937–963; (*b*) C. Tomasini, G. Angelici and N. Castellucci, *Eur. J. Org. Chem.*, 2011, 3648–3669; (*c*) G. Guichard and I. Huc, *Chem. Commun.*, 2011, **47**, 5933–5941; (*d*) W. S. Horne and S. H. Gellman, *Acc. Chem. Res.*, 2008, **41**, 1399–1408; (*e*) D. Seebach and J. Gardiner, *Acc. Chem. Res.*, 2008, **41**, 1366–1375; (*f*) J. Chatterjee, C. Gilon, A. Hoffman and H. Kessler, *Acc. Chem. Res.*, 2008, **41**, 1331–1342; (*g*) P. Maity and B. König, *Biopolymers (Pept. Sci.)*, 2008, **90**, 8–27; (*h*) D. Seebach, D. F. Hook and A. Glättli, *Biopolymers (Pept. Sci.)*, 2006, **84**, 23–37; (*i*) P. Mathur, S. Ramakumar and V. S. Chauhan, *Biopolymers (Pept. Sci.)*, 2004, **76**, 150–161; (*j*) C. Toniolo, M. Crisma, F. Formaggio and C. Peggion, *Biopolymers (Pept. Sci.)*, 2001, **60**, 396–419; (*k*) J. Venkatraman, S. C. Shankaramma and P. Balaram, *Chem. Rev.*, 2001, **101**, 3131–3152; (*l*) R. P. Cheng, S. H. Gellman and W. F. DeGrado, *Chem. Rev.*, 2001, **101**, 3219–3232; (*m*) D. J. Hill, M. J. Mio, R. B. Prince, T. S. Hughes and J. S. Moore, *Chem. Rev.*, 2001, **101**, 3893–4011.

3 P. Chakrabarti and D. Pal, *Prog. Biophys. Mol. Biol.*, 2001, **76**, 1–102.

4 M. W. MacArthur and J. M. Thornton, *J. Mol. Biol.*, 1991, **218**, 397–412.

5 G. D. Rose, L. M. Gierasch and J. A. Smith, *Adv. Protein Chem.*, 1985, **37**, 1–109.

6 (*a*) C. Armishaw, A. A. Jensen, T. Balle, R. J. Clark, K. Harpsøe, C. Skonberg, T. Liljefors and K. Strømgaard, *J. Biol. Chem.*, 2009, **284**, 9498–9512; (*b*) J. A. Tran, F. C. Tucci, M. Arellano, W. Jiang, C. W. Chen, D. Marinkovic, B. A. Fleck, J. Wen, A. C. Foster and C. Chen, *Bioorg. Med. Chem. Lett.*, 2008, **18**, 1931–1938; (*c*) E. F. Rosloniec, T. Brandstetter, S. Leyer, F.-W. Schwaiger and Z. A. Nagy, *J. Autoimmun.*, 2006, **27**, 182–195; (*d*) M. Cai, C. Cai, A. V. Mayorov, C. Xiong, C. M. Cabello, V. A. Soloshonok, J. R. Swift, D. Trivedi and V. J. Hruby, *J. Pept. Res.*, 2004, **63**, 116–131; (*e*) I. J. McFadyen, K. Sobczyk-Kojiro, M. J. Schaefer, J. C. Ho, J. R. Omnaas, H. I. Mosberg and J. R. Traynor, *J. Pharmacol. Exp. Ther.*, 2000, **295**, 960–966; (*f*) D. R. Bolin, A. L. Swain, R. Sarabu, S. J. Berthel, P. Gillespie, N. J. S. Huby, R. Makofske, L. Orzechowski, A. Perrotta, K. Toth, J. P. Cooper, N. Jiang, F. Falcioni, R. Campbell, D. Cox, D. Gaizband, C. J. Belunis, D. Vidovic, K. Ito, R. Crowther, U. Kammlott, X. Zhang, R. Palermo, D. Weber, J. Guenot, Z. Nagy and G. L. Olson, *J. Med. Chem.*, 2000, **43**, 2135–2148; (*g*) Y. Tong, Y. M. Fobian, M. Wu, N. D. Boyd and K. D. Moeller, *J. Org. Chem.*, 2000, **65**, 2484–2493; (*h*) F. Falcioni, K. Ito, D. Vidovic, C. Belunis, R. Campbell, S. J. Berthel, D. R. Bolin, P. B. Gillespie, N. Huby, G. L. Olson, R. Sarabu, J. Guenot, V. Madison, J. Hammer, F. Sinigaglia, M. Steinmetz and Z. A. Nagy, *Nat. Biotechnol.*, 1999, **17**, 562–567; (*i*) Y. Tong, Y. M. Fobian, M. Wu, N. D. Boyd and K. D. Moeller, *Bioorg. Med. Chem. Lett.*, 1998, **8**, 1679–1682.

7 (*a*) C. A. Thomas, E. R. Talaty and J. G. Bann, *Chem. Commun.*, 2009, 3366–3368; (*b*) W. Kim, K. I. Hardcastle and V. P. Conticello, *Angew. Chem., Int. Ed.*, 2006, **45**, 8141–8145; (*c*) C. M. Taylor, R. Hardré and P. J. B. Edwards, *J. Org. Chem.*, 2005, **70**, 1306–1315; (*d*) C. L. Jenkins, L. E. Bretscher, I. A. Guzei and R. T. Raines, *J. Am. Chem. Soc.*, 2003, **125**, 6422–6427; (*e*) L. Halab, F. Gosselin and W. D. Lubell, *Biopolymers (Pept. Sci.)*, 2000, **55**, 101–122; (*f*) E. Beausoleil, R. Sharma, S. W. Michnick and W. D. Lubell, *J. Org. Chem.*, 1998, **63**, 6572–6578; (*g*) J. L. Flippen-Anderson, R. Gilardi, I. L. Karle, M. H. Frey, S. J. Opella, L. M. Gierasch, M. Goodman, V. Madison and N. G. Delaney, *J. Am. Chem. Soc.*, 1983, **105**, 6609–6614; (*h*) N. G. Delaney and V. Madison, *J. Am. Chem. Soc.*, 1982, **104**, 6635–6641.

8 (*a*) K. Guitot, M. Larregola, T. K. Pradhan, J.-L. Vasse, S. Lavielle, P. Bertus, J. Szymoniak, O. Lequin and P. Karoyan, *ChemBioChem*, 2011, **12**, 1039–1042; (*b*) C. Mothes, M. Larregola, J. Quancard, N. Goasdoué, S. Lavielle, G. Chassaing, O. Lequin and P. Karoyan, *ChemBioChem*, 2010, **11**, 55–58; (*c*) J. Quancard, P. Karoyan, O. Lequin, E. Wenger, A. Aubry, S. Lavielle and G. Chassaing, *Tetrahedron Lett.*, 2004, **45**, 623–625; (*d*) P. W. Baures, W. H. Ojala, W. B. Gleason and R. L. Johnson, *J. Pept. Res.*, 1997, **50**, 1–13.

9 Torsion angles (ϕ,ψ) for an ideal βI-turn: in i+1 (–60,–30), in i+2 (–90,0); for an ideal βII-turn: in i+1 (–60,120), in i+2 (80,0). Note that they differ in the i+1 ψ and the i+2 ϕ angles, as a consequence of a ≈ 180° flip of the plane defined by the central amide group.

10 A. Aubry, M. T. Cung and M. Marraud, *J. Am. Chem. Soc.*, 1985, **107**, 7640–7647.

11 B. Castro, J. R. Dormoy, G. Evin and C. Selve, *Tetrahedron Lett.*, 1975, **14**, 1219–1222.

12 R. Bardi, A. M. Piazzesi, C. Toniolo, N. Sen, H. Balaram and P. Balaram, *Acta Crystallogr., Sect. C*, 1988, **44**, 1972–1976.

13 (*a*) A. I. Jiménez, C. Cativiela, J. Gómez-Catalán, J. J. Pérez, A. Aubry, M. París and M. Marraud, *J. Am. Chem. Soc.*, 2000, **122**, 5811–5821; (*b*) A. I. Jiménez, C. Cativiela, A. Aubry and M. Marraud, *J. Am. Chem. Soc.*, 1998, **120**, 9452–9459.

14 See the ESI‡.

15 (*a*) R. O. Gould, A. M. Gray, P. Taylor and M. D. Walkinshaw, *J. Am. Chem. Soc.*, 1985, **107**, 5921–5927; (*b*) E. Benedetti, G. Morelli, G. Némethy and H. A. Scheraga, *Int. J. Pept. Protein Res.*, 1983, **22**, 1–15.

16 M. T. Cung and M. Marraud, *Biopolymers*, 1982, **21**, 953–967.

17 The $J_{H\alpha-H\beta}$ values measured in the present work (500 MHz) for the L-Phe residue in **5** and D-Phe in **6** differ slightly from those reported in ref. 10 (100 MHz). The predicted populations of χ^1 rotamers (using the equation in ref. 16, as done in ref. 10) for the new J values are: 50% *gauche*(–) for D-Phe in **6**; 56% *gauche*(+) for L-Phe in **5**.

18 (*a*) R. Mahalakshmi, S. Raghothama and P. Balaram, *J. Am. Chem. Soc.*, 2006, **128**, 1125–1138; (*b*) E. A. Meyer, R. K. Castellano and F. Diederich, *Angew. Chem., Int. Ed.*, 2003, **42**, 1210–1250; (*c*) C. A. Hunter, J. Singh and J. M. Thornton, *J. Mol. Biol.*, 1991, **218**, 837–846; (*d*) S. K. Burley and G. A. Petsko, *Adv. Protein Chem.*, 1988, **39**, 125–189; (*e*) S. K. Burley and G. A. Petsko, *Science*, 1985, **229**, 23–28.

19 T. Ashida and M. Kakudo, *Bull. Chem. Soc. Jpn*, 1974, **47**, 1129–1133.

20 The γ and δ hydrogens of the pyrrolidine ring have been labelled as *endo* or *exo* depending on whether they are on the same or the opposite side of the ring as the carbonyl group, respectively.

21 C. A. G. Haasnoot, F. A. A. M. de Leeuw and C. Altona, *Tetrahedron*, 1980, **36**, 2783–2792. The equation including the β-effect was used.

22 The Haasnoot–Altona equation from ref. 21 was used as implemented in the free-access program MestReJ: A. Navarro-Vázquez, J. C. Cobas, F. J. Sardina, J. Casanueva and E. Diez, *J. Chem. Inf. Comput. Sci.*, 2004, **44**, 1680–1685.

23 E. Aliev and D. Courtier-Murias, *J. Phys. Chem. B*, 2007, **111**, 14034–14042.

24 J. Quancard, P. Karoyan, S. Sagan, O. Convert, S. Lavielle, G. Chassaing and O. Lequin, *Eur. J. Biochem.*, 2003, **270**, 2869–2878.

25 (*a*) G. M. Sheldrick, *SHELXS-97, Program for the Solution of Crystal Structures*, University of Göttingen: Göttingen, 1997; (*b*) G. M. Sheldrick, *SHELXL-97. Program for the Refinement of Crystal Structures*, University of Göttingen: Göttingen, 1997.